Theor Chem Acc (2004) 111:328–334
DOI 10.1007/s00214-003-0513-8

Theoretical
Chemistry Accounts

Regular article

Electrostatic interactions in peptides. Polarisation effects due to an α-helix

Xavier Assfeld[1], **Nicolas Ferré**[1,2], **Jean-Louis Rivail**[1]

[1] UMR CNRS no. 7565, Structure et réactivité des systèmes moléculaires complexes, Université Henri Poincaré, B.P. 239, 54506, Nancy-Vandoeuvre, France
[2] Dipartimento di Chimica, Università di Siena, via Aldo Moro, 2, 53100 Siena, Italy

Received: 20 December 2002 / Accepted: 25 March 2003 / Published online: 30 January 2004

Abstract. A quantum mechanical/molecular mechanical study of a dodecapeptide made of 11 alanine and one asparagine residues in a helical conformation is carried out by means of the local self-consistent field/molecular mechanical and integrated molecular orbital and molecular mechanics computational schemes. The electronic properties of the asparagine side chain are analysed to extract the influence of electrostatic and induction interaction. One finds that induction may play an important role in the energetic and structural features of the systems modelled with mixed methods. The importance of performing quantum computations which explicitly take account of the electrostatic interactions is pointed out.

Keywords: Quantum mechanical/molecular mechanical – Local self-consistent field – Integrated molecular orbital and molecular mechanics – Electrostatics – Induction

Introduction

The influence of the macromolecular surroundings on the structure and the chemical properties of part of a macromolecule is sometimes compared to the effect of a solvent [1], so it happens that, for qualitative studies, it may be simulated by a dielectric continuum [2] exactly like in the case of a liquid [3]. Nevertheless, the similarity is not perfect. In a liquid, the solvent molecules are free to orient themselves to minimise the free energy of the system. In the case of a macromolecule, the degrees of freedom of the neighbouring groups are rather limited and some local structures may be rather rigid. This is the case, in particular, of α-helices in proteins which create a strong electric field in their surroundings owing to the cooperative effect of the ordered polar peptidic bonds. Therefore, one expects some polarisation effects in the vicinity of such structures which may be different from those produced by a polar or even a nonpolar polarisable solvent.

As electrostatic interactions in proteins are considered as playing an important role in biochemical processes [4], the aim of this study is to analyse in some detail the modifications induced by electrostatic interactions on some structural features of a model system. For this purpose, we undertook a series of quantum chemical computations (quantum mechanical, QM) on an amino acid side chain interacting with a model of an α-helix. The system under consideration in this study is made of a sequence of 11 alanine residues followed by one asparagine. Two extra peptidic bonds are formed at both ends by addition of an aceto group at the N terminus and a methylamino group at the C terminus (Scheme 1). The study consists in an analysis of the variations of the geometry and charges of the amidic group of the side chain of asparagine which will act as a marker and scan the space close to the helix. The quantum chemical computation is limited to the side chain of the asparagine residue, the rest of the system being represented by a classical molecular mechanical (MM) force field within the framework of the so-called QM/MM methods [5]. There are several schemes working at the ab initio or density functional theory (DFT) level of theory used for QM/MM modelling of macromolecular systems [6]. The main difference rests in the way they treat the junction between the QM and MM subsystems. In some cases and additional monovalent atom, or "link atom" is introduced to saturate the dangling bond [7]. In other methods, the junctions are achieved by strictly localised bond orbitals (SLBOs) [8].

Contribution to the Jacopo Tomasi Honorary Issue

Correspondence to: J.-L. Rivail
e-mail: jean-louis.rivail@lctn.uhp-nancy.fr

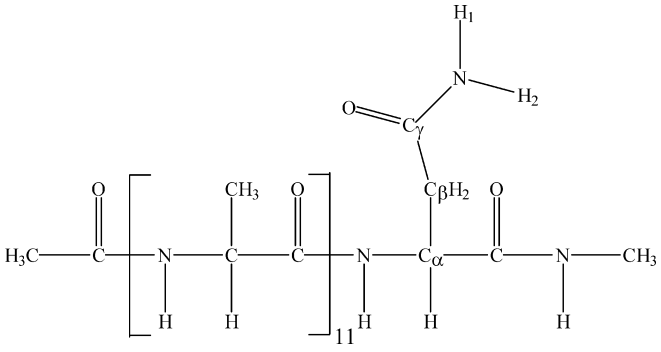

Scheme 1

In this study we mainly use one such method which we developed and which is known as the local self-consistent-field (LSCF) scheme [9, 10].

Computational methodology

The LSCF method consists of computing the Hartree–Fock or Kohn–Sham orbitals of the fragment of interest subject to the constraint of orthogonality of these orbitals to the predetermined strictly localised ones. This is achieved by expanding these orbitals on a basis of functions orthogonal to the SLBOs, derived from the basis set used for the computation [9]. The corresponding algorithm is a simple modification of the standard quantum chemical algorithms. In order to perform full geometry optimisations including the QM and the MM parts of the system, one has to carefully define the properties of the SLBOs. In the present study, the separation between the two subsystems is located at the carbon–carbon bond between the C_α atom in the main chain and the neighbouring C_β carbon atom of the side chain of asparagine. The SLBO is simply defined on an ethane model molecule by means of the Weinstein–Pauncz localisation procedure [11]. This frontier bond being a purely covalent single bond, each of the two electrons described by the SLBO compensates a nuclear charge on each atom. Therefore, the electrical neutrality is achieved by assuming that the atom at the edge of the MM part has a charge increased by 1 au. The rest of the QM/MM potential directly derives from the MM force field. The atomic charges in the MM subsystem interact with the electrons and nuclei of the QM one. This is the origin of the electrostatic and polarisation effects on which we focus our attention in this study. The changes of the SLBO during the geometry optimisation process is twofold. The orientation of the bond with respect to the molecular framework may change. The changes of the orbital are simply obtained by a standard matrix transformation. The other deformations of the bond, at a fixed orientation, are taken into account simply by normalisation. In order to optimise the full QM/MM system, the knowledge of the derivatives of the orbital is required. These derivatives are computed numerically as described in Ref. [10]. Finally, the additional energy variations, due to the atomic orbital overlap variation and to the neglect of the core–nuclei repulsion, with the length of the SLBO are defined by an empirical universal frontier bond potential [10].

An alternative QM/MM approach is made possible by the integrated molecular orbital and molecular mechanics (IMOMM) method [12], which uses a hydrogen atom as a saturating atom on the quantum part so that the bond between the quantum and the classical parts is simulated quantum mechanically by the bond with this atom, and by the true bond at the MM level. In addition, the electrostatic interactions between the quantum and the classical parts are taken into account at the MM level only. Therefore, the electronic polarisation effects of the quantum part are ignored in this approach and a comparison with the LSCF/MM method is expected to inform us of the importance of the induction effects.

In this study, the MM part is described by the Amber force field [13]. The quantum chemical computations are performed in the DFT formalism using the hybrid B3PW91 functional [14] and the standard 6-311G(d,p) basis set by means of the GAUSSIAN code [15] in which we have implemented the LSCF/MM method.

Results

Test of the method

Before starting the study, a test of the LSCF method seems useful. For this purpose we performed a full geometry optimisation at the B3PW91/6-311G(d,p) level of theory of the quantum fragment in which the dangling bond is either saturated by a hydrogen atom (acetamide), or by a methyl group (propionamide), or even is represented by the SLBO defined previously (LSCF). A fourth system is considered in which the SLBO is linked to a classical methyl group (propionamide LSCF/MM). The most relevant data are collected in Table 1. They show that the variations of the bond lengths and atomic charges from one system to another are of the same order of magnitude, and thus no further refinement of the hybrid force field will be considered here.

QM/MM study with a fixed helix geometry

A first series of QM/MM computations, performed by both LSCF/MM and IMOMM methods, was carried out at a fixed helix geometry obtained after a full optimisation of the system in its helical structure at the MM level represented in Fig. 1. The orientation of the side chain is defined by the dihedral angle χ, which is the angle between the plane formed by the carbon atom of the carbonyl group of the backbone, the C_α and C_β atoms and the plane C_α, C_β, C_γ (Scheme 1). In this optimised geometry, one finds for this angle $\chi = 75.5°$. We consider six different orientations of the asparagine side chain defined by the C_α–C_β–C_γ–N dihedral angle, which we call θ in this paper and which varies from 0 to 300° in steps of 60°. In the MM optimised structure, $\theta = 325.2°$. The other degrees of freedom of the side chain are optimised by the LSCF/MM method, still at the B3PW91/6-311G(d,p) level of theory. A seventh structure is obtained by leaving the θ free to vary and the minimum is reached for a value of 346.5°. The main

Table 1. Bond lengths and Mulliken atomic charges of the oxygen and nitrogen atoms of the amide functional group belonging to the side chain of the asparagine residue

System	Bond lengths (Å)		Atomic charges (au)	
	$N–C_\gamma$	$C_\gamma=O$	q_N	q_O
Acetamide	1.360	1.214	–0.476	–0.375
Propionamide	1.364	1.210	–0.476	–0.373
LSCF	1.375	1.214	–0.462	–0.373
PropionamideLSCF/MM	1.373	1.215	–0.463	–0.374

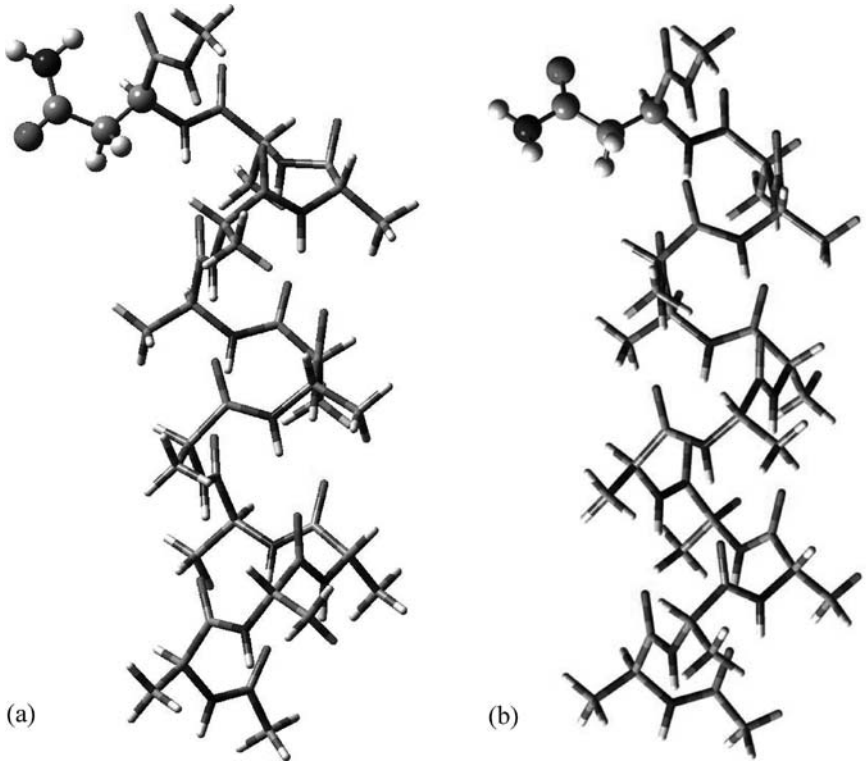

Fig. 1. a Fully optimised structure of the peptide at the local self-consistent field (*LSCF*)/molecular mechanical (*MM*) level of theory. **b** Optimised side chain at the LSCF/MM level of theory after a rotation of $\theta = 180°$ (see text). The quantum mechanical part is sketched with balls and sticks, and the MM one with tubes

Table 2. Main geometric features for various orientations of the side chain of the asparagine residue. Bond lengths in angstroms, angles in degrees

	Angle θ[a]						
	0	60	120	180	240	300	346.5[b]
$N–C_\gamma$	1.366	1.374	1.375	1.380	1.371	1.369	1.363
$C_\gamma=O$	1.219	1.215	1.211	1.211	1.213	1.217	1.220
$\angle C_\beta–C_\gamma–N$	119.6	116.5	114.0	112.9	115.0	117.0	119.5
$\angle O=C_\gamma–N$	121.6	121.6	121.4	121.1	122.0	121.7	121.6

[a]See text
[b]LSCF/MM optimised value

geometric features are given in Table 2. The IMOMM study consists in single-point computations on the previous structures. Finally, in order to evaluate the magnitude of the electrostatic interactions, two other series of single-point computations were performed by both the LSCF/MM and the IMOMM methods on the previous structures in which the charges of the classical part were set to zero. The difference of this energy and the corresponding QM/MM energy at the same geometry gives the electrostatic plus induction energy of interaction of the quantum subsystem (side chain) with the rest of the molecule (helix) in the LSCF/MM study. It only gives a classical electrostatic contribution with the IMOMM results. The relative variations of the energy of the whole system, obtained on the same geometries by the full MM, LSCF/MM and IMOMM computations are represented in Fig. 2. The electrostatic plus induction energy of interaction of the quantum fragment with the helix (LSCF) and the electrostatic energy (IMOMM) for these various structures are given in Table 3. The Mulliken charges of the oxygen and nitrogen atoms and of the groups of atoms of the side chain, obtained by both methods, are given in Table 4, together with their variations when the classical charges are set to zero, for the LSCF/MM method only since these charges do not vary in the IMOMM method.

Fully optimised structures

In order to complete the study, a full optimisation of the system with the LSCF/MM method was performed followed by a single-point computation with the classical charges set to zero. For comparison, the results of a full optimisation with the IMOMM method are also considered. Finally, another optimised structure with only one constraint, θ fixed at 180°, i.e. close to the value corresponding to the maximum energy value of the internal rotation energy curve, computed with the LSCF/MM method is also considered. In this case, apart from a slight torsion of the axis of the helix, no noticeable changes are observed compared with the previous case where the helix was rigid, so we shall not comment on this result any further.

The root-mean-square deviation of the atom coordinates between the various optimised structures are the following:

- Amber-IMOMM: 0.268 Å.
- Amber-LSCF/MM: 0.354 Å.
- LSCF/MM-IMOMM: 0.181 Å.

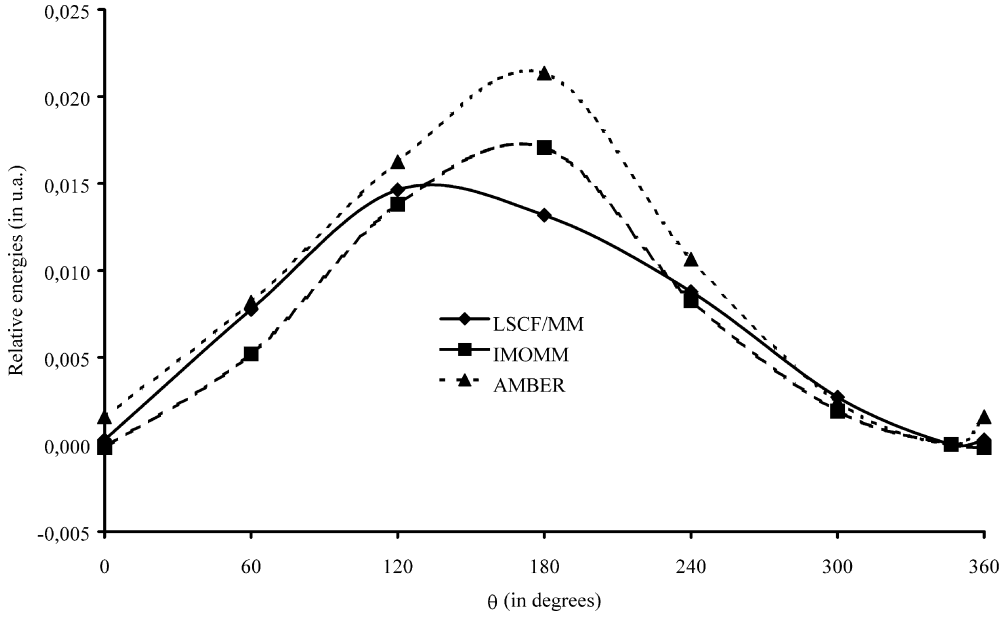

Fig. 2. Relative energy variations with the dihedral angle, θ, (see text)

Table 3. Influence of the classical charges on the quantum mechanical energy

Method	Angle θ[a]						
	0	60	120	180	240	300	346.5[b]
LSCF/MM	–0.2241	–0.2150	–0.2068	–0.2071	–0.2127	–0.2231	–0.2247
IMOMM	–0.1035	–0.0950	–0.0860	–0.0852	–0.0915	–0.1015	–0.1035

[a]See text
[b]LSCF/MM optimised value

Table 4. Mulliken atomic charges (atomic units) of the oxygen and nitrogen atoms and of the groups of atoms of the asparagine side chain

Method		Angle θ[a]						
		0	60	120	180	240	300	346.5[b]
IMOMM	q_O	–0.376	–0.359	–0.363	–0.358	–0.365	–0.364	–0.378
LSCF/MM	q_O	–0.398	–0.374	–0.358	–0.359	–0.379	–0.384	–0.400
	Δq_O[c]	–0.011	–0.004	0.021	0.023	0.003	–0.010	–0.011
IMOMM	q_N	–0.457	–0.438	–0.462	–0.452	–0.454	–0.445	–0.463
LSCF/MM	q_N	–0.484	–0.443	–0.470	–0.465	–0.461	–0.470	–0.491
	Δq_N[c]	–0.023	0.000	–0.006	–0.006	–0.004	–0.019	–0.024
IMOMM	q_{CO}	–0.071	–0.068	–O.056	–0.055	–0.064	–0.070	–0.068
LSCF/MM	q_{CO}	–0.104	–0.073	–0.043	–0.051	–0.062	–0.089	–0.102
	Δq_{CO}[c]	–0.0007	0.008	0.031	0.032	0.019	–0.008	–0.008
IMOMM	q_{NH2}	0.004	0.014	–0.001	0.001	0.004	0.014	0.003
LSCF/MM	q_{NH2}	0.021	0.010	–0.023	–0.025	–0.006	0.028	0.021
	Δq_{NH2}[c]	0.042	0.018	–0.008	–0.010	0.004	0.037	0.043
IMOMM	q_{CH2}	–0.050	–0.0080	–0.096	–0.103	–0.093	–0.076	–0.054
LSCF/MM	q_{CH2}	0.121	0.094	0.087	0.104	0.089	0.094	0.119
	Δq_{CH2}[c]	–0.020	–0.015	–0.014	–0.013	–0.013	–0.016	–0.019

[a]See text
[b]LSCF/MM optimised value
[c]Differences between the Mulliken atomic charges obtained at the LSCF/MM level and the same charges obtained with the classical charges set to zero

The relevant geometric parameters of the amide functional group of the side chain of the fully optimised structures are given in Table 5, and the Mulliken atomic charges of the corresponding atoms are collected in Table 6.

Detailed study of the side chain–helix electrostatic interaction

In order to analyse the possible cooperative effects of the ordered amino acids of the α-helix, a series of

Table 5. Relevant geometric parameters of the side chain of the asparagine residue in the fully optimised geometries. Bond lengths are in angsroms, bond angles and dihedral angles in degrees

	$C_\gamma=O$	C_γ–N	O–C_γ–N	C_β–C_γ–N	χ^a	θ^a
AMBER	1.218	1.311	118.3	120.6	75.5	325.2
IMOMM	1.215	1.372	121.7	117.8	68.6	360.5
LSCF/MM	1.222	1.366	121.0	119.6	71.7	345.9

[a]See text

Table 6. Mulliken atomic charges (atomic units) for the amide functional group of the asparagine residue. Δq corresponds to the variation of the Mulliken charge when the classical charges are set to zero

		C_γ	O	N	H_1	H_2
IMOMM	q	0.299	–0.368	–0.451	0.232	0.221
LSCF/MM	q	0.279	–0.418	–0.495	0.210	0.292
	Δq	–0.011	–0.028	–0.033	–0.019	0.079

single-point QM/MM computations were performed on systems in which the classical charges of the alanine residues were progressively set to zero, starting from the N-terminus alanine (number 1), and including each time one more residue in the process, until the classical main chain of asparagine (residue number 12) was discharged. The Amber classical charges were adjusted in order to make each amino acid electrically neutral. In our model, neither the aceto group at the N terminus nor the methylamino group at the C terminus is neutral, but the sum of their charges is zero so, in this study, the charges of both end groups are not modified. The study was performed on two systems in which the helix had the MM optimised structure and in which the side chain was optimised at the LSCF/MM level at the energy minimum geometry and after a rotation corresponding to $\theta = 180°$. The relative variations of the charge of the CO, NH_2 and CH_2 groups during the progressive cancellation of the electrostatic interaction are represented in Figs. 3 and 4.

Discussion

The standard solvent effect on amides is an electron shift from the donor amino group to the acceptor carbonyl one. The charge shift is accompanied by a shortening of the C–N bond and an increase of the C = O bond length [16]. The situation here is quite different. Compared with the free amide group, the geometry of the side chain does not change much: the O–C–N angle is reduced by 0.1° and, in contrast to the case of the solution, both C–N and C = 0 bond lengths increase slightly. This different behaviour is more visible if one compares the atomic charges obtained at the optimised geometry with and without the charges on the classical atoms (Table 5) The effect of the electrostatic interactions is a nonnegligible increase of the negative charge of both nitrogen and oxygen atoms, which is mainly compensated by an increase of the positive charge of the hydrogen atom bound to a carbonyl group of the helix by a hydrogen bond and as a consequence of an increase of the global charge of the NH_2 group.

Another interesting observation arises from the comparison of the effect of the classical charges on the total energy in the LSCF/MM computations and the IMOMM ones. The energy variations include both the electrostatic and induction energies in the first case and the pure Amber electrostatic energy in the second one. One notices that there is a ratio greater than 2 between both quantities. The difference is even more pronounced when the structures are fully optimised. In the LSCF/MM scheme the electrostatic plus induction contribution amounts to −0.3032 au. The classical Amber electrostatic contribution given by IMOMM is only −0.1162 au. for the same structure and reaches −0.1166 au for the IMOMM fully optimised one. This clearly shows that electronic polarisation effects are important, in particular if one remembers the fact that the atomic charges are quite large in the Amber force field. For instance the charge of the oxygen atom in a peptidic bond is −0.5679 (to be compared with the Mulliken charge found lower than −0.5 in every case) and the carbon atom is given a charge of 0.5973 (to be compared with about 0.3).

The analysis of the variations of the atomic charges in the presence of the classical charges of the force field gives more insight into the inductive effects. In the fully optimised structure, the increase of the electron population on the carbonyl group and on the nitrogen atom clearly indicates that this part of the side chain is in a region where the electrostatic potential is positive. This is still true in the other low-energy structures, in particular when θ takes the values 0 and 300°. Conversely, in the high-energy structures ($\theta = 120$, 180 and 240°), the electronic population of these local components is reduced under the influence of the charges of the helix. This is particularly visible on the oxygen atom. Obviously this means that these conformations of the side chain are not favourable from the point of view of electrostatic interactions, and this remark is confirmed by the variations of the Amber electrostatic interaction energy. This feature can be understood if one keeps in mind that the dipole moment of an amide is roughly oriented along the N...O direction with a negative end at the oxygen atom. On the other hand, the global dipole of an α-helix has its positive end at the N terminus and the negative one at the C terminus. In the low-energy structure shown in Fig. 1, which is stabilised mainly by the hydrogen bond between the quantum hydrogen atom of the NH_2 group and the classical carbonyl group of the main chain, it appears that orientation of the side chain is also the most favourable one among the possibilities allowed by the chemical bonds. The Mulliken charges computed at the IMOMM and LSCF/MM levels are close within the error bars and they roughly show the same variations, especially if one takes into

account that they correspond to slightly different geometries and that the induction effects are absent in the former. The largest difference in the absolute values of these charges is observed for the CH_2 group, but this is obviously due to the fact that this group is bonded to a hydrogen link atom in the IMOMM scheme and to the localised orbital in the LSCF/MM one.

The inductive effects, which are difficult to extract, play, as usual, a stabilising role in every conformation. This property is probably the main explanation of the differences observed in Fig. 2 between the curve corresponding to the LSCF/MM data, which include induction, and the IMOMM and Amber ones, which do not. Induced polarisation is an important phenomenon. For instance, the Mulliken charge of the oxygen atom on the side chain varies by more than 0.06 au when this side chain rotates around the C_β–C_γ bond and the variations of the charge of the nitrogen atom are almost as large. These effects are absent in the IMOMM scheme but are easily accessible with the LSCF/MM method.

The cooperative effects of the various amino acids of the helix can be analysed in Figs. 3 and 4. The variation of the charges is monotonous until alanine 7. It becomes larger when the charges of alanine 8, which is the first residue of the loop containing the asparagine, are cancelled. The maximum variations are observed when alanine 9 is included in the charge switching off process and then there is a change of sign in the slope for

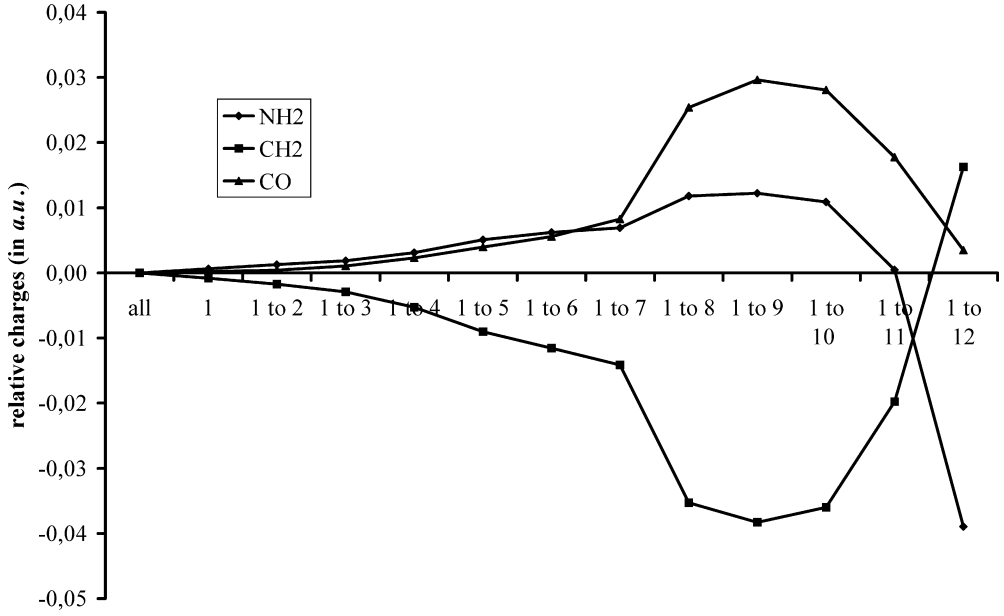

Fig. 3. Relative charge variations of the CO, NH_2, and CH_2 groups with respect to the zeroing of the point charges of the residues of the helix for the minimum energy conformation

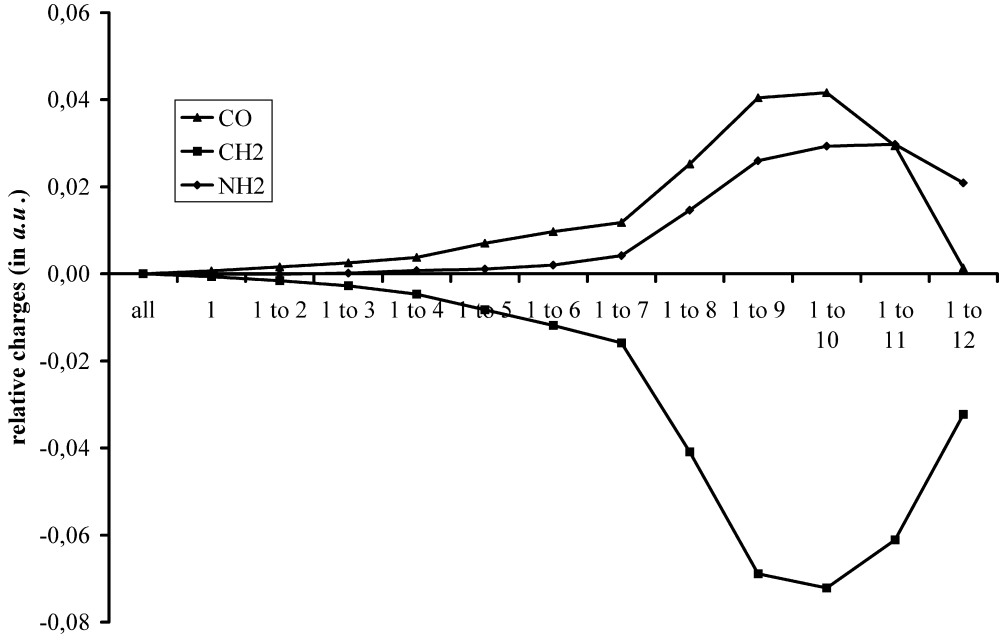

Fig. 4. Relative charge variations of the CO, NH_2, and CH_2 groups with respect to the zeroing of the point charges of the residues of the helix for the conformation corresponding to $\theta = 180°$

residues 10 and 11, indicating a different interaction with the residues of the loop. As expected, cancelling the charges of the main chain of asparagine has the strongest influence on the charges of the side chain, especially on the NH_2 group in the fully optimised structure, owing to the cancelling of the hydrogen bond. This variation is far less pronounced in the $\theta = 180°$ structure in which the hydrogen bond is absent. Finally, one notices that the variations of the charges of the CO and NH_2 groups under the electrostatic influence of the alanine residues are qualitatively similar: they both increase their electronic population and these variations are compensated by those of the CH_2 group, which is the electron-donating one.

Regarding the geometric features, the optimised structures obtained by the IMOMM and LSCF/MM methods are rather close, but they depart to a slightly greater extent from the structure given by the pure MM approach with the Amber force field. However, as far as the quantum subsystem is concerned, the bond lengths and angles obtained with the LSCM/MM method, given in Table 5, are closer to the Amber data (and seem slightly more realistic) than the IMOMM ones.

Conclusion

By combining the results of computations performed with various methods, this study allowed us to evaluate the role of electrostatic and induction interactions on the structure and properties of a fragment of a polypeptide. These effects are, as expected, far from negligible and one should be careful when choosing a method to select the proper one which will provide reliable data for the chemical problem of interest. In particular, if one is interested in computing local properties which depend on the electronic density, it is compulsory to use a computational scheme which accounts for induction effects. In the case of large systems, this can only be achieved by QM/MM computations, but, in addition, the QM computation must include the perturbation by the classical charges into the Hamiltonian. Among the possible methods available, the LSCF/MM scheme seems quite convenient and the present study is another successful test of this method.

Acknowledgements. This work was done with the financial support of the Université Henri Poincaré and CNRS. Computational facilities of the Centre Informatique National de l'Enseignement Supérieur are gratefully acknowledged. The authors thank Christophe Chipot for providing them with the initial MM optimised dodecaalanine structure.

References

1. Warshel A (1991) Computer modeling of chemical reactions in enzymes and solutions. Wiley, New York
2. Archontis G, Simonson T (2001) J Am Chem Soc 123:11047
3. Tomasi J, Persico M (1994) Chem Rev 94:2027
4. Warshel A (2000) Theor Chem Acc 103:337
5. Gao J (1996) Rev Comput Chem 7:119
6. Field M J (2002) J Comput Chem 23:48
7. Field M J, Bash PA, Karplus M (1990) J Comput Chem 11:700
8. (a) Thery V, Rinaldi D, Rivail J-L, Maigret B, Ferenczy GG (1994) J Comput Chem 15:269; (b) Monard G, Loos M, Thery V, Baka K, Rivail J-L (1996) Int J Quantum Chem 58:153
9. Assfeld X, Rivail J-L (1996) Chem Phys Lett 263:100
10. Ferré N, Assfeld X, Rivail J-L (2002) J Comput Chem 23:610
11. Weinstein H, Pauncz R, Cohen M (1971) Adv At Mol Phys 7:97
12. (a) Maseras F, Morokuma K (1995) J Comput Chem 16:1170; (b) Humbel S, Sieber S, Morokuma K (1996) J Chem Phys 105:1959
13. Cornell WD, Cieplak P, Bayly CI, Gould IR, Merz KM Jr, Fergusson DM, Spellmeyer DC, Fox T, Caldwell JW, Kollman PA (1995) J Am Chem Soc 117:5179
14. (a) Becke AD (1993) J Chem Phys 98:5648; (b) Perdew JP, Burke K, Wang Y (1996) Phys Rev B 54:16533
15. Frisch MJ, Trucks GW, Schlegel HB, Scuseria GE, Robb MA, Cheeseman JR, Zakrzewski VG, Montgomery JA Jr, Stratmann RE, Burant JC, Dapprich S, Millam JM, Daniels AD, Kudin KN, Strain MC, Farkas O, Tomasi J, Barone V, Cossi M, Cammi R, Mennucci B, Pomelli C, Adamo C, Clifford S, Ochterski J, Petersson GA, Ayala PY, Cui Q, Morokuma K, Malick DK, Rabuck AD, Raghavachari K, Foresman JB, Cioslowski J, Ortiz JV, Baboul AG, Stefanov BB, Liu G, Liashenko A, Piskorz P, Komaromi I, Gomperts R, Martin RL, Fox DJ, Keith T, Al-Laham MA, Peng CY, Nanayakkara A, Challacombe M, Gill PMW, Johnson B, Chen W, Wong MW, Andres JL, Gonzalez C, Head-Gordon M, Replogle ES, Pople JA (1998) Gaussian 98, revision A.9. Gaussian, Pittsburgh, PA
16. Dillet V, Rinaldi D, Rivail J-L (1994) J Phys Chem 98:5034